Enhancement of Corrosion Protection Effect in Polyaniline via the Formation of Polyaniline−Clay Nanocomposite Materials

Jui-Ming Yeh,* Shir-Joe Liou, Chiung-Yu Lai, and Pei-Chi Wu

Department of Chemistry, Chung-Yuan Christian University, Chung Li, Taiwan 320, ROC

Tsung-Yen Tsai

Union Chemical Laboratories, Industrial Technology Research Institute, Hsinchu, Taiwan 300, ROC

Received November 28, 2000. Revised Manuscript Received January 23, 2001

A series of nanocomposite materials that consisted of emeraldine base of polyaniline and layered montmorillonite (MMT) clay were prepared by effectively dispersing the inorganic nanolayers of MMT clay in organic polyaniline matrix via in-situ polymerization. Organic aniline monomers were first intercalated into the interlayer regions of organophilic clay hosts and followed by an one-step oxidative polymerization. The as-synthesized polyaniline−clay lamellar nanocomposite materials were characterized by infrared spectroscopy, wide-angle powder X-ray diffraction, and transmission electron microscopy. Polyaniline−clay nanocomposites (PCN) in the form of coatings with low clay loading (e.g., 0.75 wt %) on cold-rolled steel (CRS) were found much superior in corrosion protection over those of conventional polyaniline based on a series of electrochemical measurements of corrosion potential, polarization resistance, and corrosion current in 5 wt % aqueous NaCl electrolyte. The molecular weights of polyaniline extracted from PCN materials and bulk polyaniline were determined by gel permeation chromatography (GPC). Effects of the material composition on the gas barrier property, thermal stability, and mechanical strength of polyaniline along with PCN materials, in the form of both fine powder and free-standing film, were also studied by gas permeability measurements, differential scanning calorimetry, thermogravimetric analysis, and dynamic mechanical analysis.

Introduction

Conducting polymers, such as polypyrrole, polythiophene, polyaniline, etc., consisted of conjugated electronic structures have received considerable attention lately because of many promising technological applications. Some specific conducting polymers, e.g., polyaniline and its derivatives, have been found to display interesting corrosion protection properties. In the past decade, the use of polyanilines as anticorrosion coatings had been explored as the potential candidates to replace the chromium-containing materials, which have adverse health and environmental concerns.[1−6] Wei et al.[6] demonstrated the corrosion protection effect of polyaniline through a series of electrochemical measurements on the doped or undoped polyaniline-coated cold rolled steel (CRS) under various conditions. Wessling[5] claimed a full mechanism that the corrosion protection of polyaniline on steel is attributed to an increase in the corrosion potential and to the redox catalytic property of polyaniline in the formation of passive layer of metal oxide.

Layered materials, such as smectite clays (e.g., montmorillonite, MMT), attracted intense research interest for the preparation of polymer−clay nanocomposites in the past decade, because of their lamellar elements displayed high in-plane strength, stiffness as well as high aspect ratio.[7] The polymer−clay nanocomposites were found to enhance the gas barrier,[8] thermal stability,[9] mechanical strength,[10] and fire-retardant[11] properties of polymers. Recently, there are a number of reports on the preparation and properties for the lamellar nanocomposites of polyaniline with various layered materials.[12−18]

* To whom correspondence should be addressed.

(1) Deberry, D. W. *J. Electrochem. Soc.* **1985**, *132*, 1027.
(2) Wessling, B. *Synth. Met.* **1991**, 907, 1057.
(3) Elsenbaumer, R. L.; Lu, W. K.; Wessling, B. *Int. Conf. Synth. Met.*, Seoul, Korea, Abstract No. APL(POL)1-2, 1994.
(4) Wrobleski, D. A.; Benicewicz, B. C.; Thompson, K. G.; Byran, C. J. *Polym. Prepr. (Am. Chem. Soc., Div. Polym. Chem.)* **1994**, *35* (1), 265.
(5) Wessling, B. *Adv. Mater.* **1994**, *6*, 226.
(6) Wei, Y.; Wang, J.; Jia, X.; Yeh, J.-M.; Spellane, P. *Polymer* **1995**, *36*, 4535.
(7) Pinnavaia, T. J. *Science* **1983**, *220*, 365.
(8) Lan, T.; Kaviratna, P. D.; Pinnavaia, T. J. *Chem. Mater.* **1994**, *6*, 573.
(9) Tyan, H.-L.; Liu, Y.-C.; Wei, K.-H. *Chem. Mater.* **1999**, *11*, 1942.
(10) Wang, Z.; Pinnavaia, T. J. *Chem. Mater.* **1998**, *10*, 3769.
(11) Gilman, J. W.; Jackson, C. L.; Morgan, A. B.; Hayyis, R., Jr.; Manias, E.; Giannelis, E. P.; Wuthenow, M.; Hilton, D.; Phillips, S. H. *Chem. Mater.* **2000**, *12*, 1866.
(12) Biswas, M.; Ray, S. S. *J. Appl. Polym. Sci.* **2000**, *77*, 2948.

10.1021/cm000938r CCC: $20.00
Published on Web 02/28/2001

In this paper, we present the first evaluation of corrosion protection effect for the polyaniline−clay nanocomposite (PCN) materials on CRS in comparison with that of the emeraldine base of polyaniline by performing a series of electrochemical measurements of corrosion potential, polarization resistance, and corrosion current in 5 wt % aqueous NaCl electrolyte. The PCN materials were characterized by Fourier transform infrared spectroscopy (FTIR), wide-angle powder X-ray diffraction (WAXRD), and transmission electron microscopy (TEM). Gel permeation chromatography (GPC) was employed to determine the molecular weight of extracted polyaniline from the PCN materials and bulk polyaniline. The effect of material composition on the gas molecular barrier property, thermal stability, and mechanical strength was also investigated by the gas permeability measurements, thermogravimetric analysis (TGA), differential scanning calorimetry (DSC), and dynamic mechanical analysis (DMA).

Experimental Section

Chemicals and Instrumentations. Aniline (99%, Fluka) was doubly distilled under a reduced pressure. Both 1.0 M HCl and 1.0 M NH_4OH were prepared from diluting the concentrated ammonia and hydrochloric acid (Riedel-de Haen) with distilled water for preparing the acidic and basic aqueous media, respectively. 1-Methyl-2-pyrrolidinone (NMP) (99.97%, Tedia) was used as received without further purification. Ammonium persulfate (98%, SHOWA) was employed as oxidant. The montmorillonite clay employed in this study had a unit cell formula $Na^{+}_{0.31}[Al_{1.67}Mg_{0.33}]Si_4O_{10}(OH)_2 \cdot 5.8H_2O$ and a CEC value of 122 mequiv/100 g. The structure of intercalating agent was $C_{11}H_{23}CONH(CH_2)_2N^{+}(CH_3)_2CH_2CHOHCH_2SO_3^{-}$ (cocamidopropylhydroxysultaine). Both the clay and intercalating agent were supplied by Industrial Technology Research Institute (ITRI), Taiwan.

Wide-angle X-ray diffraction study of the samples was performed on a Rigaku D/MAX-3C OD-2988N X-ray diffractometer with cooper target and Ni filter at a scanning rate of 4°/min. The samples for transmission electron microscopy (TEM) study was first prepared by putting powder of PCN materials into epoxy resin capsules followed by curing the epoxy resin at 100 °C for 24 h in a vacuum oven. Then the cured epoxy resin containing PCN materials were microtomed with a Reichert-Jumg Ultracut-E into 60−90 nm thick slices. Subsequently, one layer of carbon about 10 nm thick was deposited on these slices on mesh 100 copper nets for TEM observations on a JEOL-200FX with an acceleration voltage of 120 kV.

Electrochemical measurements of sample-coated CRS coupons were performed on a VoltaLab 21 potentiostat/galvanostat in a standard corrosion cell equipped with two graphite rod counter electrodes and a saturated calomel electrode (SCE) as well as the working electrode. The dynamic mechanical analyses for the free-standing film of samples were carrying out from 30 to 280 °C with a Perkin-Elmer DMA 7e analyzer at a heating rate of 5 °C at a fixed frequency of 1 Hz. A Perkin-Elmer thermal analysis system equipped with model 7 DSC and model 7/DX TGA was employed for the thermal analyses under air or nitrogen flow. The programmed heating rate was 20 °C/min in most cases. The molecular weight of polymer extracted from all composite samples as well as bulk polyaniline was determined on a Waters GPC model 2 II equipped with a model 590 programmable solvent delivery module, a differential refractometer detector, and a Styragel HT column with NMP as eluant and monodispersed polystyrenes as calibration standards. FTIR spectra were recorded on pressed KBr pellets using a BIO-RAD FTS-7 FTIR spectrometer.

Synthesis of Polyaniline. In a typical procedure, 10 mL of doubly distilled aniline (0.107 mol) was dissolved in 600 mL of 1.0 M HCl, and the mixture was precooled to ∼0 °C in an ice bath. A solution (200 mL) of 5.6 g (0.025 mol) of $(NH_4)_2S_2O_8$ in 1.0 M HCl was added to the aniline solution dropwise over a period of 15 min with vigorously magnetic stirring. After ∼2 h, the precipitate was collected on a Buchner funnel. Upon drying under dynamic vacuum at room temperature, the HCl-doped polyaniline was obtained as a green powder. The HCl-doped polyaniline was subsequently converted into emeraldine base form of polyaniline by stirring ∼3 g of the emeraldine hydrochloride fine powder in an excess amount (500 mL) of 1.0 M ammonium hydroxide at room temperature for 3 h. Upon filtering and drying under dynamic vacuum for 48 h, the emeraldine base (EB) form of polyaniline was obtained as a blue powder.

Preparation of Organophilic Clay. The organophilic clay was prepared by a cation-exchange reaction between the sodium cations of MMT clay and alkylammonium ions of intercalating agent, cocamidopropylhydroxysultaine. Typically, 5 g of MMT clay with a CEC value of 122 mequiv/100 g was stirred in 500 mL of distilled water (beaker A) at room temperature overnight. A separate solution containing 2.5 g of intercalating agent in another 100 mL of distilled water (beaker B) under magnetically stirring, followed by adding 1.0 M HCl aqueous solution to adjust the pH value to about 3−4. After stirring for 1 h, the protonated amino acid solution (beaker B) was added at a rate of approximately 10 mL/min with vigorous stirring to the MMT suspension (beaker A). The mixture was stirred overnight at room temperature. The organophilic clay was recovered by ultracentrifugating (9000 rpm, 30 min) and filtering the solution in a Buchner funnel. Purification of products was performing by washing and filtering samples repeatedly for at least three times to remove any excess of ammonium ions.

Preparation of Polyaniline/Clay Nanocomposite Materials. As a typical procedure for the preparation of the PCN materials, first, an appropriate amount of organophilic clay was introduced into 400 mL of 1.0 M HCl under magnetically stirring overnight at room temperature. Aniline monomer (0.1 mol) was subsequently added to the solution which was stirred for another 24 h. Upon addition of ammonium persulfate (0.025 mol) in 20 mL of 1.0 M HCl, the solution was stirred for 3 h at 5 °C in an ice bath. The as-synthesized HCl-doped lamellar nanocomposite precipitates were then obtained by filtering and drying under dynamic vacuum at room temperature for 48 h. The final PCN products in base form were obtained by immersing the HCl-doped nanocomposites into 400 mL of 1.0 M NH_4OH under magnetically stirring for 4 h at room temperature, followed by filtration and drying under vacuum at room temperature for 48 h.

Polymer Recovery (Extraction). A reverse cationic-exchange reaction was employed to separate bound polyaniline from inorganic component in the nanocomposite.[22] As a typical extraction procedure, 2 g of fine powder of as-synthesized polyaniline−clay nanocomposite was dissolved in ∼100 mL of methanol (beaker A). Separately, 10 mL of stock solution of 1 wt % $LiCl_{(s)}$ in methanol was prepared (beaker B). Both beakers were under vigorous magnetically stirring for 3−4 h

(13) Wu, C.-G.; DeGroot, D. C.; Marcy, H. O.; Schindler, J. L.; Kannewurf, C. R.; Liu,Y.-J.; Hirpo, W.; Kanatzidis, M. G. *Chem. Mater.* **1996**, *8*, 1992.
(14) Wang, L.; Brazis, P.; Rocci, M.; Kannewurf, C. R.; Kanatzidis, M. G. *Chem. Mater.* **1998**, *10*, 3298.
(15) Chao, K.-J.; Ho, S.-Y.; Chang, T.-C. US Patent 5,340,500, 1994.
(16) Giannelis, E.; Mehrota, V. US Patent 5,032,547, 1991.
(17) Choi, H. J.; Kim, J. W.; Kim, S. G.; Kim, B. H.; Joo, J. *Polym. Mater. Sci. Eng.* **2000**, *82*, 245.
(18) Wu, Q.; Xue, Z.; Qi, Z.; Wang, F. *Polymer* **2000**, *41*, 2029.
(19) Yano, K.; Usuki, A.; Okada, A. *J. Polym. Sci., Polym. Chem. Ed.* **1997**, *35*, 2289.
(20) Barber, G. D.; Moore, R. B. *Polym. Mater. Sci. Eng.* **2000**, *82*, 241.
(21) Wei, Y.; Jang, G.-W.; Hsueh, K. F.; Scherr, E. M.; MacDiarmid, A. G.; Epstein, A. J. *Polymer* **1992**, *33*, 314.
(22) Meier, L. P.; Sheldon, R. A.; Caseri, W. R.; Suter, U. W. *Macromolecules* **1994**, *27*, 1637.

Table 1. Relations of the Composition of Polyaniline (PANI)−MMT Clay Nonocomposite Materials with the E_{corr}, R_p, i_{corr}, and R_{corr} Measured from Electrochemical Methods[a]

compound code	feed composition (wt %)		inorganic content found in product[b] (wt %)	electrochemical corrosion measurements			
	polyaniline	MMT		E_{corr} (mV)	R_p (kΩ·cm^2)	i_{corr} (μA/cm^2)	R_{corr} (MPY)
bare				−641	0.8	44.4	86.1
PANI	100	0	0	−590	3.4	12.0	23.3
CLAN025	99.75	0.25	0.70	−581	13.7	2.9	5.6
CLAN05	99.50	0.50	1.50	−568	15.4	2.7	5.2
CLAN075	99.25	0.75	3.80	−555	20.0	2.4	4.5
CLAN1	99.00	1.00	4.70	−551	36.2	1.1	2.1
CLAN3	97.00	3.00	7.10	−543	57.9	0.5	1.0

[a] Saturated calomel electrode was employed as reference electrode. [b] As determined from TGA measurements.

at room temperature. After combining the contents of the two beakers, the mixture was stirred for an additional 24 h followed by Soxhlet extraction at 85−90 °C for 48 h. Extract solution was evaporated on a rotavapor under a reduced pressure at 50 °C to yield polyaniline fine powders. Molecular weights of both extracted polyaniline and bulk polyaniline were determined by gel permeation chromatography analyses with NMP as eluant.

Preparation of Coatings and Electrochemical Measurements. The EB of polyaniline and PCN fine powder were dissolved in NMP to give typically 1 wt % solutions. The solutions were cast dropwise onto the cold rolled steel (CRS) coupons (1.0 × 1.0 cm) followed by drying in air for 48 h to give coatings of ca. ∼20 μm in thickness. The coated and uncoated coupons were then mounted to the working electrode so that only the coated side of the coupon was in direct contact with the electrolyte. The edges of the coupons were sealed with super fast epoxy cement (SPAR). All the electrochemical measurements were made at room temperature and repeated at least three times. The electrolyte was NaCl (5 wt %) aqueous solution. The open circuit potential (OCP) at the equilibrium state of the system was recorded as the corrosion potential (E_{corr} in V vs SCE). The polarization resistance (R_p in Ω/cm^2) was measured by sweeping the applied potential from 20 mV below to 20 mV above the E_{corr} at a scan rate of 500 mV/min and recording the corresponding current change. The R_p value was obtained from the slope of the potential−current plot. The Tafel plots were obtained by scanning potential from 250 mV below to 250 mV above the E_{corr} at a scan rate of 500 mV/min. The corrosion current (i_{corr}) was determined by superimposing a straight line along the linear portion of the cathodic or anodic curve and extrapolating it through E_{corr}. The corrosion rate (R_{corr}, in milliinches per year, MPY) was calculated from the following equation:

$$R_{corr}\ (\mathrm{MPY}) = [0.13 i_{corr}(\mathrm{EW})]/[Ad]$$

where EW is the equivalent weight (in g/equiv), A is the area (in cm^2), and d is the density (in g/cm^3).

Preparation of Free-Standing Films and Barrier Property Measurements. A 0.3 g sample of polyaniline and PCN materials in base form was dissolved in 10 mL of NMP under magnetically stirring at room temperature for 4 h. The solution was cast onto a substrate (e.g., a microscope glass slide). The solvent was allowed to evaporate at 90−100 °C under the hood for 24 h. The sample-coated glass substrate was then immersed into the distilled water for 5−6 h to give the free-standing film of polyaniline and PCN materials. The molecular barrier of free-standing film of samples was determined by air transmission through the nanocomposite films according to ASTM standard E 96. A Yanagimoto Co., Ltd., gas permeability-measuring apparatus (model GTR 10) was employed to perform the permeation experiment of air. The pressure on one face of the free-standing film was kept at 200 kPa, and the other face was at zero pressure initially to allow the air to permeate through the free-standing film. The rate of transmission of air was obtained by gas chromatography, from which the air permeability was calculated.

Results and Discussion

The base forms of polyaniline can be schematically represented by the following general formula:

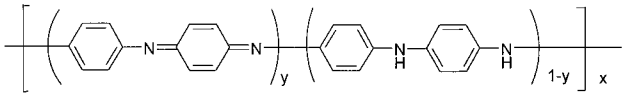

where the y value ranges from 1 for the fully oxidized polymer (so-called pernigraniline) to 0.5 for the half-oxidized polymer (emeraldine) and to 0 for the fully reduced polymer (leucoemeraldine). On the other hand, montmorillonite (MMT) is a clay mineral containing stacked silicate sheets measuring ∼10 Å in thickness and ∼2180 Å in length.[19] It possesses a high aspect ratio (about 220) and a platey morphology. The chemical structures of MMT consist of two fused silica tetrahedral sheets sandwiching an edge-shared octahedral sheet of either magnesium or aluminum hydroxide. The Na^+ and Ca^{2+} residing in the interlayer regions can be replaced by organic cations such as alkylammonium ions by an cationic-exchange reaction to render the hydrophilic layered silicate organophilic. MMT has a high swelling capacity, which is important for efficient intercalation of the polymer, and is composed of stacked silicate sheets that offer enhanced thermal stability, mechanical strength, fire-retardant, and molecular barrier properties.

To synthesize the PCN materials, organophilic clay was first prepared by a cation-exchange reaction between the sodium cations of MMT clay and alkylammonium ions of cocamidopropylhydroxysultaine. Organic aniline monomers were subsequently intercalated into the interlayer regions of organophilic clay hosts and followed by an one-step oxidative polymerization. The composition of the PCN materials was varied from 0 to 3 wt % of clay with respect to polyaniline content as summarized in Table 1.

Characterization. The representative FTIR spectra of the organophilic clay, bulk polyaniline, and PCN materials are shown in Figure 1. The characteristic vibration bands of polyaniline are at 1498 and 1583 cm^{-1}, and those of MMT clay are shown at 1040 cm^{-1} (Si−O), 600 cm^{-1} (Al−O), and 420 cm^{-1} (Mg−O).[17] As the loading of MMT clay is increased, the intensities of MMT clay bands become stronger in the FTIR spectra of PCN materials. Figure 2 shows the wide-angle powder X-ray diffraction patterns of organophilic clay and a series of PCN materials. There is a lack of any diffraction peak in $2\theta = 2-10°$ as opposed to the diffraction peak at $2\theta = 3.9°$ (d spacing = 2.26 nm) for

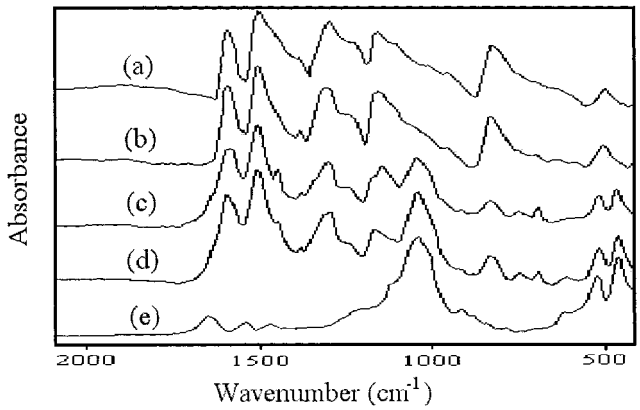

Figure 1. FTIR spectra of (a) PANI, (b) CLAN05, (c) CLAN1, (d) CLAN 3, and (e) organophilic clay.

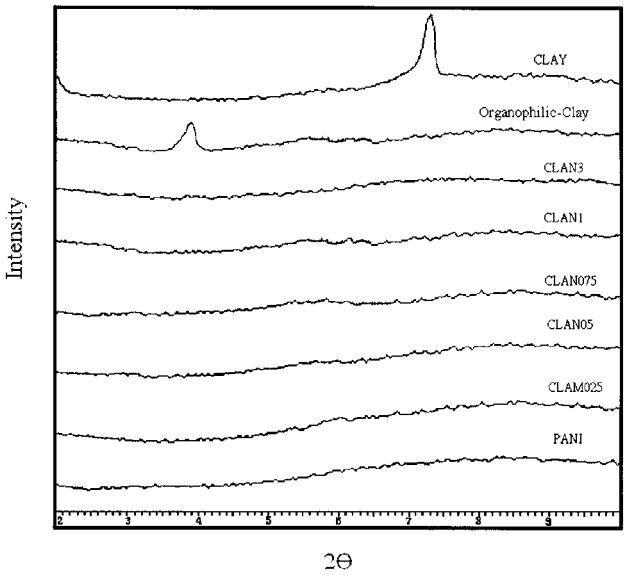

Figure 2. Wide-angle powder X-ray diffraction patterns of organophilic clay, polyaniline, and a series of polyaniline−clay nanocomposite materials.

organophilic clay, indicating the possibility of having exfoliated silicate nanolayers of organophilic clay dispersed in a polyaniline matrix.

In Figure 3, the TEM of PCN materials with 3 wt % clay loading shows that the lamellar nanocomposite has a mixed nanomorphology. Individual silicate layers, along with two, three, and four layer stacks, were found to be exfoliated in the polyaniline matrix. In addition, some larger intercalated tactoids (multilayer particles) can also be identified.

***M*$_w$ Determination of Extracted Polymers from PCN Materials and Bulk Polyaniline.** Molecular weights of the various polymer samples recovered from the nanolayers of MMT clays were obtained by gel permeation chromatography analyses. The THF-extractable component for all samples exhibited very low molecular weight (e.g., <500). The GPC elution pattern of the NMP-soluble component displayed a single peak, corresponding to high molecular weight values, as summarized in Table 2. The molecular weights of extracted polyaniline were found significantly lower than that of the bulk polyaniline, indicating the structurally restricted polymerization conditions in the intragallery region of the MMT clay[13] and/or the nature

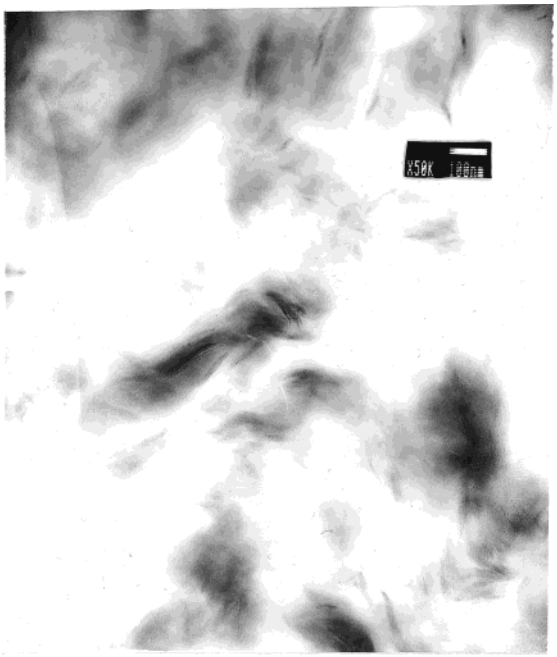

Figure 3. TEM of CLAN3: with exfoliated single, double, and triple layers and a multilayer tactoid.

Table 2. Molecular Weights of Bulk and Extracted Polyaniline

material	M_w	M_n	polydispersity
bulk polyaniline	76 700	10100	7.6
CLAN025	40 800	7100	5.7
CLAN05	38 000	6800	5.6
CLAN075	30 000	5200	5.8
CLAN1	18 200	4700	3.9
CLAN3	15 000	3900	3.8

of clay−oligomer interactions, such as adsorption, during the polymerization reaction.

Corrosion Protection Properties of Coatings. Corrosion protection of sample-coated CRS coupons can be observed from the values of corrosion potential (E_{corr}), polarization resistance (R_p), corrosion current (i_{corr}), and corrosion rate (R_{corr}), as listed in Table 1. The CRS coupon coated with EB of polyaniline shows a higher E_{corr} value than the uncoated CRS, which is consistent with previous observations.[6] However, it exhibits a lower E_{corr} value than the specimen coated with PCN materials. For example, the CLAN075-coated CRS has a high corrosion potential of ca. −555 mV at 30 min. Even after 5 h measurement, the potential remained at ca. −560 mV. Such a E_{corr} value implies that the CLAN075-coated CRS is more noble toward the electrochemical corrosion compared to the EB of polyaniline. The CLAN075-coated CRS shows a polarization resistance (R_p) value of 2.00×10^4 Ω/cm^2 in 5 wt % NaCl, which is about 2 orders of magnitude greater than the uncoated CRS.

The Tafel plots for (a) uncoated, (b) PANI-coated, (c) CLAN025-coated, (d) CLAN05-coated, and (e) CLAN075-coated CRS are shown in Figure 4. For example, the corrosion current (i_{corr}) of CLAN075-coated CRS is ca. 2.4 μA/cm^2, which is correspondent to a corrosion rate (R_{corr}) of ca. 4.46 milliinches per year (MPY) (Table 1). Electrochemical corrosion current values of PCN materials as coatings on CRS were found to decrease gradually with further increase in clay loading. Visual

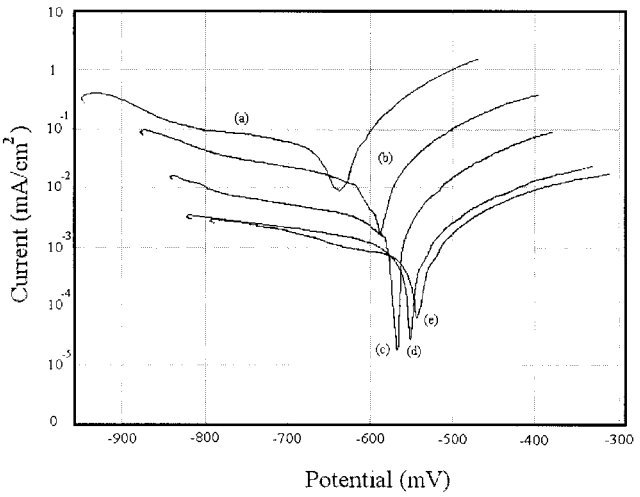

Figure 4. Tafel plots for (a) uncoated, (b) PANI-coated, (c) CLAN025-coated, (d) CLAN05-coated, and (e) CLAN075-coated CRS measured in 5 wt % NaCl aqueous solution.

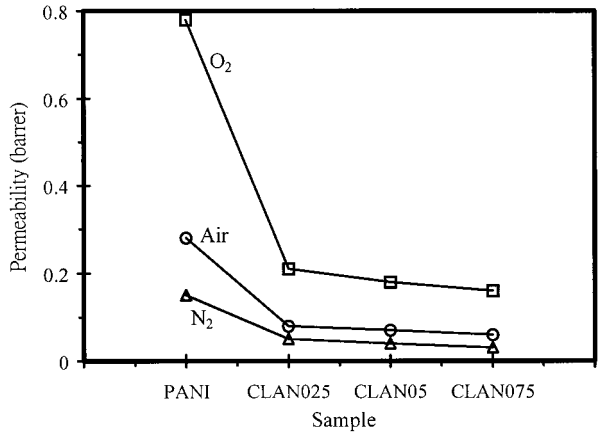

Figure 5. Permeability of O_2, N_2, and air as a function of the MMT clay content in the polyaniline−clay nanocomposite materials.

observation of the corrosion products clearly reveals that the PCN samples exhibiting corrosion protection have a grayish oxide layer form over the bare exposed CRS surface, similar to what was observed by Wessling under the polyaniline dispersion coatings on steel.[5] Enhanced corrosion protection effect of polyaniline−clay nanocomposite materials compared to bulk polyaniline might be resulted from dispersing silicate nanolayers of clay in polyaniline matrix to increase the tortousity of diffusion pathway of oxygen gas. This is further evidenced by the studies of the O_2 gas barrier effect as discussed in the following section.

Gas Barrier and Mechanical Properties of Free-Standing Films. The free-standing films of PCN materials and bulk polyaniline used for the gas barrier measurements were prepared to have film thickness of ~70 μm. Compared to polyaniline, free-standing film of PCN materials at low clay loading (e.g., 0.25 wt %) shows about 400% reduction of air, O_2, and N_2 permeability, as shown in Figure 5. This is caused by the barrier properties of the nanolayers of clay dispersed in the composite.[8] Furthermore, it should be noted that a further increase of clay loading results in a slightly enhanced gas barrier property of bulk PCN materials. In addition, we found that the free-standing film of PCN

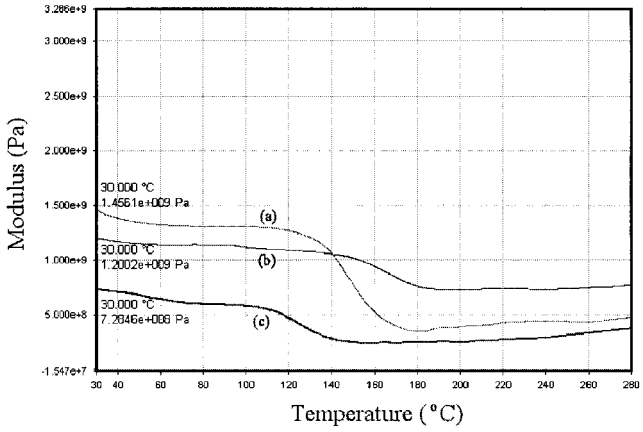

Figure 6. Relationship between the storage modulus (E') and temperature as obtained from DMA measurements on the free-standing films of (a) PANI, (b) CLAN05, and (c) CLAN075.

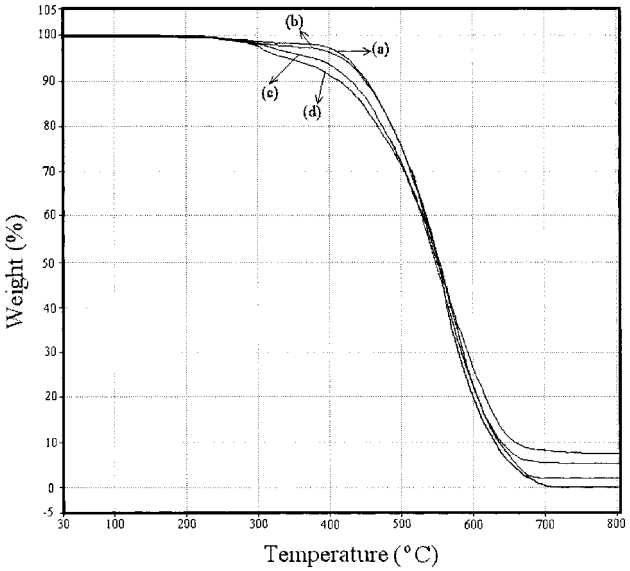

Figure 7. TGA curves of (a) PANI, (b) CLAN05, (c) CLAN1, and (d) CLAN3.

materials could not be obtained as the clay loading in the nanocomposite is increased up to 1 wt % feed ratio. The failure of free-standing film formation of PCN materials at the clay loading greater than 0.75 wt %, i.e., CLAN075, might be attributed to the observed large decrease in the molecular weight of extracted polyaniline, which leads to a significant lowering of mechanical strength. As shown in Figure 6, the moduli of the PCN free-standing films with 0.5 wt % ($E' = 1.2 \times 10^9$ Pa) and 0.75 wt % ($E' = 7.3 \times 10^8$ Pa) clay loading (Figure 6b,c) at room temperature (30 °C) are lower than the polyaniline ($E' = 1.5 \times 10^9$ Pa) (Figure 6a). Generally, there is a major suppression in the storage modulus (E') starting around 110−120 °C, which might be related to the glass transition of polyaniline.[21]

Thermal Properties of Fine Powders. Figure 7 shows typical TGA curves of the PCN materials as well as that of polyaniline, as measured under an air atmosphere. In general, there appeared to be several stages of weight loss starting at ~250 °C and ending at 800 °C, which might be correspondent to the degradation of intercalating agent followed by the structural decomposition of the polymers. According to the published reports on polymer−clay nanocomposite materi-

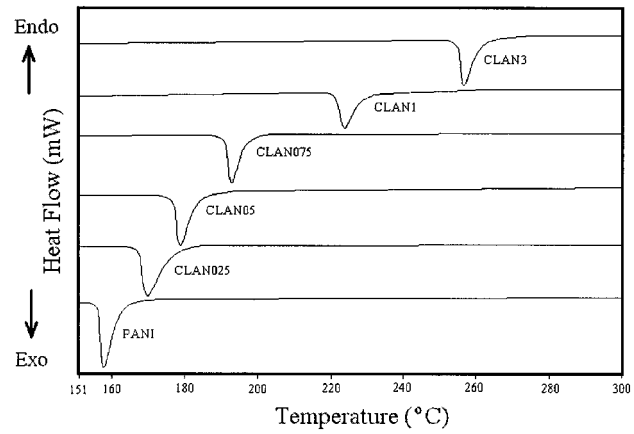

Figure 8. DSC curves of polyaniline and a series of polyaniline−clay nanocomposite materials.

als, the unparalleled ability of smectite clays was found to boost the thermal stability of polymers.[9] However, in this study, the incorporation of MMT clay into polyaniline matrix resulted in a small decrease of decomposition temperature relative to pure polyaniline. Again, this might be attributed to a significantly decreased molecular weight of extracted polyanilines compared to bulk polyaniline, reflecting a decreased temperature of thermal decomposition. After ~700 °C, the curve all became flat and mainly the inorganic residue (i.e., Al_2O_3, MgO, SiO_2) remained. From the amounts of the residue at 700 °C, the inorganic contents in the original PCN materials can be obtained, which were significantly higher than the values calculated from the feed composition (Table 1). The calculated inorganic contents tend to be lower than those determined from TGA probably because of low yield of polyaniline prepared from aniline monomers in PCN materials. We also found from DSC measurements as in Figure 8 that the incorporation of MMT clay into polyaniline resulted in a large increase in the crystalline temperature (heating scan) relative to pure polyaniline. This behavior was expected and associated with the strong heterogeneous nucleation effect of the large clay particles in the PCN system.[20] As the loading of MMT clay is increased, the crystalline temperature of PCN materials became higher.

Concluding Remarks

The corrosion protection effect of polyaniline−clay nanocomposite (PCN) materials at low clay loading compared to conventional polyaniline was demonstrated by a series of electrochemical measurements of corrosion potential, polarization resistance, and corrosion current on CRS in 5 wt % aqueous NaCl electrolyte. The coatings of PCN materials were found to offer good corrosion protection and showed a better anticorrosion performance than conventional polyaniline coating. The as-synthesized PCN materials were characterized by FTIR, wide-angle powder X-ray diffraction and TEM. The molecular weights of polyaniline extracted from lamellar PCN materials are lower than the bulk polyaniline, indicating the structurally restricted polymerization conditions in the intragallery region of the MMT clay. The gas barrier property, thermal stability, and mechanical strength were also investigated by the gas permeability measurements, TGA, DSC, and DMA. The O_2 gas barrier of PCN materials in the form of free-standing film (e.g., CLAN025) exhibits a 400% reduction in permeability compared to conventional polyaniline. However, the incorporation of nanolayers of MMT clay in polyaniline matrix resulted in a decrease in mechanical strength (in the form of free-standing films) and in thermal decomposition temperature (in the form of fine powders) based on the DMA and TGA studies. This might be attributed to the significantly decreased molecular weight of polyanilines formed in the MMT clay. Dispersed nanolayers of MMT clays in polyaniline−clay nanocomposite materials led to a significant increase of crystalline temperature based on the DSC results.

Acknowledgment. The financial support of this research by the NSC 89-2113-M-033-001 is gratefully acknowledged.

CM000938R